Abridged version

KAWASAKI STEEL TECHNICAL REPORT
No.8 (September 1983)

Production of Ultra-Low Carbon Steel by Combined Process of Bottom-Blown Converter and RH Degasser

Norio Sumida, Tetsuya Fujii, Yukio Oguchi, Hitoshi Morishita, Keisuke Yoshimura, Fumio Sudo

Synopsis :
A method for producing ultra-low carbon steel with carbon content 20 ppm or less was investigated, and a highly efficient and yet economic manufacturing process using the combination of bottom-blown converter and RH vacuum degasser was established. First, the decarburizing reaction in the RH vacuum degasser was analyzed using a reaction model, and the relationship between operational conditions and the rate of decarburization was elucidated. On the basis of the analytic results, it was attempted to improve operational conditions for the decarburizartion under vacuum, and a technique to reduce the carbon concentration to 20 ppm or less within 10-15 min. of the decarburization treatment in RH was established. It is expected that the combination of the ultra-low carbon steel manufacturing process and the continuous annealing (KM-CAL) technique would greatly contribute to the production of cold rolled steel sheet having excellent mechanical properties such as of extra-deep drawing steel and deep drawing high strength steel.

The body can be viewed from the next page.

KAWASAKI STEEL TECHNICAL REPORT No. 8 September 1983

Production of Ultra-Low Carbon Steel by Combined Process of Bottom-Blown Converter and RH Degasser*

Norio SUMIDA** Tetsuya FUJII** Yukio OGUCHI**
Hitoshi MORISHITA*** Keisuke YOSHIMURA*** Fumio SUDO***

A method for producing ultra-low carbon steel with carbon content 20 ppm or less was investigated, and a highly efficient and yet economic manufacturing process using the combination of bottom-blown converter and RH vacuum degasser was established. First, the decarburizing reaction in the RH vacuum degasser was analyzed using a reaction model, and the relationship between operational conditions and the rate of decarburization was elucidated. On the basis of the analytic results, it was attempted to improve operational conditions for the decarburization under vacuum, and a technique to reduce the carbon concentration to 20 ppm or less within 10–15 min. of the decarburization treatment in RH was established.

It is expected that the combination of the ultra-low carbon steel manufacturing process and the continuous annealing (KM-CAL) technique would greatly contribute to the production of cold rolled steel sheet having excellent mechanical properties such as of extra-deep drawing steel and deep drawing high strength steel.

1 Introduction

To meet an increasing demand for cold rolled steel sheets of improved mechanical properties, and to cope with the change of annealing process from batch-type to continuous, it is urgently desired to establish a technique for making ultra-low carbon steel. Particularly, for an economical manufacture of extra-deep drawing cold rolled steel sheet or high-tensile strength cold rolled steel sheet of excellent deep-drawing properties, it is essential to obtain ultra-low carbon molten steel with carbon concentration lower than 20 ppm in the steelmaking process.

The ultra-low carbon molten steel is produced by decarburizing molten steel in the converter to carbon concentration about 300 ppm, and then by the vacuum decarburization in the RH circulating vacuum degasser (to be abbreviated as RH hereinafter) under reduced partial pressure of CO gas through the reaction C + O → CO (gas). The production of ultra-low carbon steel involves a problem that the vacuum decarburization to the desired level of carbon content takes so long a time as to cause a drop in steel temperature and an effort to compensate the temperature drop by an increased tapping temperature of converter will result in a higher steelmaking cost including that for refractory material. On the other hand, reducing the carbon content in steel just before tapping so as to shorten the time required for the vacuum decarburization in RH will increase the oxidation loss of iron, lowering the steel yield. Moreover, a considerably long processing line after tapping causes difficulty in performing the continuous-continuous casting.

In the bottom-blown converter at Chiba Works of Kawasaki Steel all the refining oxygen gas is blown-in from the bottom to agitate molten steel intensively, allowing decarburization to an adequately low level of carbon content while suppressing the oxidation loss of steel bath, in comparison with the conventional top-blown converter. The present report discusses a technique highly efficient and economical in making the ultra-low carbon steel through the vacuum decarburization in RH of molten steel of 100–200 ppm carbon content derived from the bottom-blown converter.

2 Analysis for Increasing Decarburization Reaction Rate

A method of increasing vacuum decarburization

* Originally published in *Kawasaki Steel Giho*, 15 (1983) 2, pp. 60–65
** Chiba Works
*** Research Laboratories

rate in RH was analyzed by using a mathematical model so as to obtain basic data for determining optimum equipment dimensions and operational procedures[1].

A reaction model used for the analysis is shown in **Fig. 1**. In designing the model, the following assumptions were made.

(1) Molten steel is perfectly mixed in both ladle and vacuum vessel.
(2) The decarburization reaction proceeds in the vacuum vessel only.
(3) The rate of decarburization reaction is proportional to carbon concentration in molten steel and controlled by the mass transfer of carbon in molten steel.

According to the tracer experiment to be described later using radioactive isotopes, the assumption (1) is pertinent. As for (2), the results of the authors' experiment[2] with RH having three snorkels proved that the contribution of decarburization reaction in the up-legs to the total reaction was less than 10% and most of the decarburization proceeded in the vacuum vessel. The assumption (3) is considered reasonable since the oxygen concentration in the ultra-low carbon region is a few times as high as the carbon concentration, and the partial pressure of CO in the gas phase is lower than 1 mmHg.

The mass balance of carbon in the ladle and the vacuum vessel under the conditions (1) to (3) is represented by eqs. **(1)** and **(2)**.

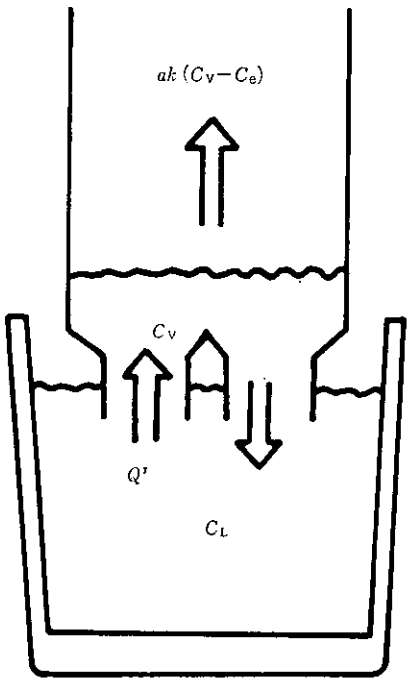

Fig. 1 Decarburization model for calculation

$$V\frac{dC_L}{dt} = Q'(C_V - C_L) \quad \cdots\cdots\cdots\cdots\cdots (1)$$

$$v\frac{dC_V}{dt} = Q'(C_L - C_V) - ak(C_V - C_e) \quad \cdots (2)$$

Initial conditions are

$$C_L = C_V = C_L^0, \text{ at } t = 0 \quad \cdots\cdots\cdots\cdots (3)$$

V and v: Volume of molten steel(m^3) in ladle and vacuum vessel, respectively

ak: Volumetric coefficient for decarburization reaction (m^3/min)

C_L, C_V: Carbon concentration(%) in ladle and vacuum vessel, respectively

C_L^0: Carbon concentration (%) before treatment

C_e: Carbon concentration(%) in molten steel in equilibrium with partial pressure of CO in gas phase

Q': Circulation flow rate of molten steel (m^3/min)

t: time(min)

If eqs. **(1)** and **(2)** are solved under the conditions given by eq. **(3)** assuming that $C_e \fallingdotseq 0$, eqs. **(4)** and **(5)** are obtained as approximate solutions.

$$C_L = C_L^0 \cdot \exp(-Kt) \quad \cdots\cdots\cdots\cdots\cdots (4)$$

$$K = \frac{Q'}{V} \cdot \frac{ak}{Q' + ak} \quad \cdots\cdots\cdots\cdots\cdots (5)$$

It has been known that the measured values of carbon concentration in the ladle can apparently be reduced on the basis of the first order reaction rate equation. The eq. **(4)** agrees with the previous findings.

The effects of circulation rate, Q', and volumetric coefficient, ak, of reaction on the reaction rate of decarburization are examined for two extreme cases of reaction control and circulation control. The reaction control refers to the condition in which the circulation rate of molten steel is adequately high and the overall reaction rate of decarburization, that is, the time change of C_L, is controlled by the decarburization rate within the vacuum vessel. On the other hand, the circulation control refers to the condition in which the reaction of decarburization in the vacuum vessel is sufficiently rapid and the overall decarburization rate is controlled by the circulation rate. Corresponding to these rate determining steps, eqs. **(4)** and **(5)** may be rewritten as eqs. **(6)** and **(7)**, respectively.

Reaction control:

$$C_L = C_L^0 \cdot \exp(-akt/V) \quad \cdots (6)$$

Circulation control:

$$C_L = C_L^0 \cdot \exp(-Q't/V) \quad \cdots (7)$$

That is, C_L is determined by ak alone in case of reaction control, and by Q' alone in case of circulation control.

The effects of Q and ak to the apparent rate constant K are calculated by using eq. **(4)** and shown in **Fig. 2.** The figure shows the presence of three regions: ① K increases little by increasing Q (equal to Q' with unit converted to t/min) (reaction control), ② K increases little by increasing ak (circulation control), and ③ K affected equally by Q and ak (mixed control). The improvement of the operational conditions to increase K and to shorten the decarburization time can be investigated on the basis of **Fig. 2.**

3 Experiment for Increasing Decarburization Rate

Ⅰ, Ⅱ and Ⅲ in **Fig. 2** represent three phases of experiment for increasing the decarburization rate. In the beginning of the experiment, the conditions were in the phase Ⅰ. As the size of the snorkel was expanded to increase Q, the conditions were improved to phase Ⅱ. Finally, as ak was augmented by agitating molten steel in the vacuum vessel more vigorously and increasing the interfacial reaction area between gas and molten metal, the conditions were improved to phase Ⅲ. The experiments to increase the decarburization rate will be described below.

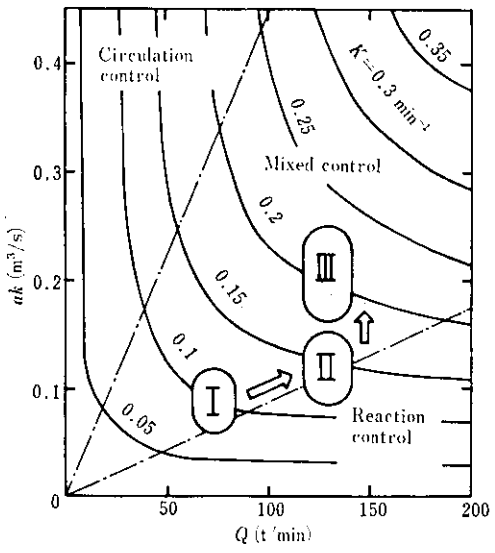

Fig. 2 Effects on K of circulating flow rate, Q, and volumetric coefficient of mass transfer of carbon, ak

3.1 Experiment for Increasing Circulation Rate

3.1.1 Measurement of circulation rate

The analysis described in the preceding section allows the quantitization of the effect of circulation rate on the decarburization rate. However, the previous measurement of circulation rate mostly concerned small-sized RH[2-6] and only a few data were available on the modern large-sized snorkel. For this reason, the circulation rate of molten steel was measured by using radioactive isotopes (RI)[7].

The measuring method shown in **Fig. 3** is the peak area method[8] which is nearly equal to the conventional one. Three units of RH were used for the experiment: No. 3 of Chiba Works, and Nos. 1 and 2 of Mizushima Works. The experimental conditions are shown in **Table 1.**

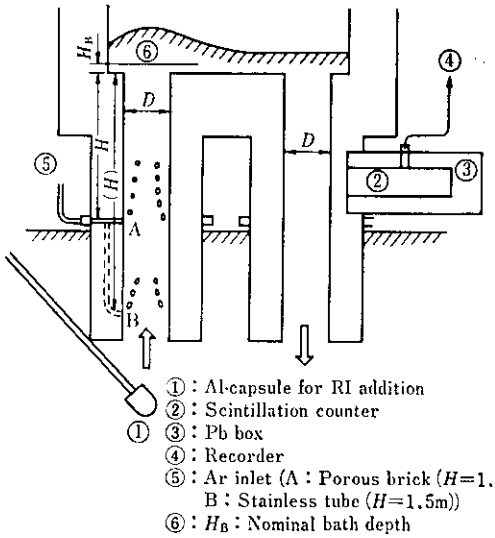

Fig. 3 RH degasser and arrangement for measuring circulation flow rate

Table 1 Experimental conditions for measurement of circulating flow rate

RH degasser	Chiba No. 3	Mizushima No. 1	Mizushima No. 2
Ladle capacity (t)	240	200	280
Inner dia. of snorkel, D (cm)	45	30~40	36~45
Ar flow rate, G (Nl/min)	300~1 500	400~1 700	500~2 000
Nominal bath depth in vacuum vessel, H_B (cm)	-17~20	0~15	0~15
Operational pressure, P_V (Torr)	0.5~20	0.5~20	0.5~20
Ar inlet (A: Porous brick (H=1.2 m) B: Stainless tube (H=1.5 m))	A, B	A, B	B

3.1.2 Results and discussion

Examples of radio activity measurement by using a scintillation counter are shown in **Fig. 4**. On the basis of these data, the circulation rate was calculated with eq. **(8)**.

$$Q = \frac{W(I_2 - I_1)}{\int_{t_1}^{t_2} \{I(t) - I_1\}\,dt} \quad \cdots\cdots\cdots\cdots\cdots\cdots (8)$$

Q: Circulation rate(t/min)
W: Molten steel treated(t)
I_1 and I_2: Intensity of radioactivity(cps) before the addition and after uniform mixing of RI, respectively
t_1 and t_2: time(s) when intensity of radioactivity starts to increase, and time(s) giving the minimum radioactivity after the peak, respectively
$I(t)$: intensity of radioactivity(cps) at time t

The relationship of blown-in Ar gas flow rate, G, to circulation flow rate, Q, is shown in **Fig. 5**.[7] When G is greater than 800 N*l*/min, the effect of G on Q is small, tending to be saturated. The calculated values plotted in the same figure coincide well with the measured values for the snorkel of diameter, $D = 30$ cm, though about 20 t/min smaller than the measured values for the large-sized snorkel of $D = 45$ cm. As for the method of blowing Ar gas in, no significant difference was recognized between the stainless steel pipe and the porous brick. Moreover, it was found that the degree of vacuum in the chamber had no effect on the circulation rate, so long as the pressure was between 0.3 mmHg and 20 mmHg.

Figure 6 shows the relationship of cross-sectional area, A, of snorkel to the circulation rate, Q (t/min), for the cases of G greater than 800 N*l*/min. From this figure, it is evident that Q is proportional to A, that is, even when the snorkel diameter is increased, the efficiency of the air lift pump is apparently not reduced in the way it is by the uneven distribution of Ar gas bubbles. Concurrently with the measurement of circulation rate, the time required for perfect mixing of molten steel in the ladle was determined on the basis of time changes in the intensity of radioactivity within the ladle. In case of No. 3 RH, Chiba Works, the time was 2 min.

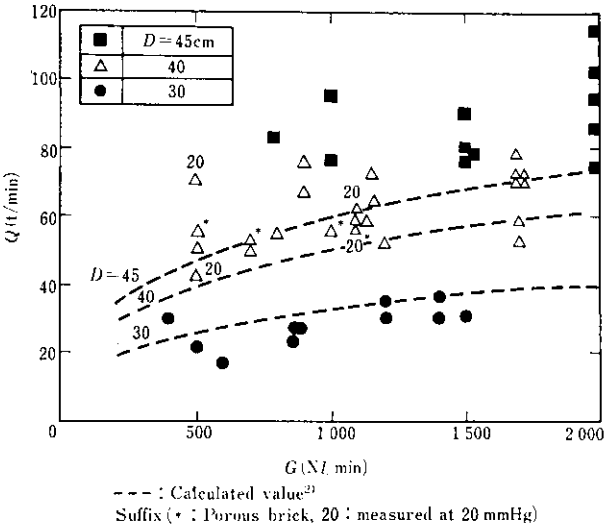

Fig. 5 Relation between Ar gas flow rate, G, and Q

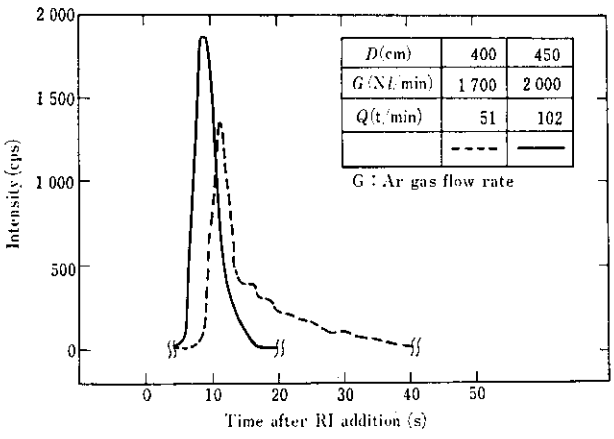

Fig. 4 An example of radio activity measurement

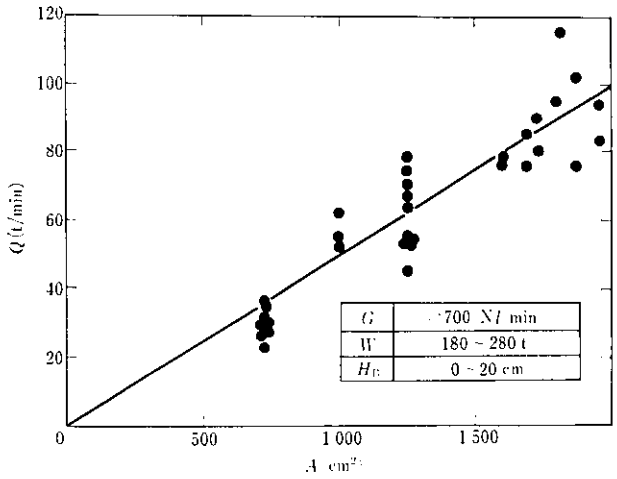

Fig. 6 Relation between cross-sectional area of snorkel A and Q

3.2 Experiment for Increasing Decarburization Rate

3.2.1 Snorkel diameter and increase of Ar gas flow rate

At the time of starting the experiment for making ultra-low carbon steel, snorkel diameter was 45 cm and Ar gas flow rate 1 000–1 500 Nl/min as the operating conditions. As shown in **Fig. 2** ①, the apparent rate constant, K, of the decarburization reaction was within the range between 0.08 min^{-1} and 0.10 min^{-1}. Under these conditions, it took about 30 min. to obtain rimmed steel of less than 20 ppm carbon concentration. To cope with this, it is necessary to set the temperature of steel tapped from the converter to 1 680°C or higher, which poses problems in respect of production efficiency and cost.

For the purpose of solving these problems, it was attemped first to increase Q on the basis of **Fig. 2**, with the snorkel diameter and the Ar gas flow rate set at 600 mm and 2 000–2 500 Nl/min, respectively. Consequently, K became 0.09–0.15 min^{-1}, being improved to ② in **Fig. 2**.

Through these improvements, molten steel of 200 ppm initial carbon concentration was decarburized to 10–33 ppm within 20 min. of the decarburization treatment in RH. In making ultra-low carbon steels of 20 ppm or less carbon content, however, there were some cases of requiring more than 20 min. decarburization treatment, therefore, further improvement for increasing the decarburization rate was required.

3.2.2 Experiment of adding H_2 gas

According to **Fig. 2**, ② is located at the boundary between reaction control and circulation control regions. It was considered difficult, therefore, to increase the K-value greater than the present through the increase of circulation rate alone. For this reason, a method was sought for whereby the volumetric coefficient, ak, of decarburization reaction was increased through a more vigorous agitation of molten steel in the vacuum chamber, and an increased interfacial area for reaction between gas and molten metal.

Since the depth of molten steel in the vacuum vessel determined by the static pressure balance was as small as 100–200 mm, it seemed difficult to augment the agitation of molten steel in the vessel by increasing circulation gas flow. It was attempted, therefore, to achieve more vigorous agitation of molten steel and increase the interfacial area for reaction through boiling of hydrogen in the vacuum vessel by feeding hydrogen gas into molten steel in the ladle and supplying molten steel of higher hydrogen concentration to the vacuum vessel.

For the H_2-feeding experiment, the feeding rate of hydrogen gas required for improving the decarburization rate was calculated as described below.

Generally, the decarburization reaction proceeds apparently in the form of first order reaction, but in the vicinity of a 30 ppm carbon concentration the decarburization rate drops abruptly, transposing into the form of the reaction rate equation of higher order. Since the partial pressure of CO in the gas phase was sufficiently low, it was difficult to attribute this drop in rate to the approach to the equilibrium. This phenomenon seemed to be due to a decrease in evolution of CO gas owing to the reduction of carbon concentration, apparently caused by the lowered agitation of molten steel in the vacuum vessel through the suppression of CO boiling and the reduced interfacial area for reaction. If the H_2 gas generation was maintained at the level corresponding to the rate of CO gas production in the region of 30 ppm or higher carbon concentration until the concentration was reduced to 20 ppm, it would be possible to prevent the decrease of decarburization rate and to increase the K-value. The hydrogen concentration in molten steel and the rate of H_2 gas supply for meeting this requirement were estimated as described below.

The apparent rate equations of decarburization and dehydrogenation are given by **(9)** and **(10)**, respectively.

$$\frac{dC_C}{dt} = -K_C \cdot C_C \quad \cdots\cdots\cdots\cdots\cdots\cdots\cdots\cdots (9)$$

$$\frac{dC_H}{dt} = -K_H \cdot C_H \quad \cdots\cdots\cdots\cdots\cdots\cdots\cdots\cdots (10)$$

Using the measured values, the apparent rate constants for decarburization and dehydrogenation are determined to be $K_C = 0.12\,min^{-1}$ and $K_H = 0.16\,min^{-1}$ (see **Fig. 8**). The hydrogen concentration, C_H, at which the rate of H_2 gas generation is equal to that of CO gas generation at the carbon concentration, $C_C = 30$ ppm, is calculated as $C_H = 3.1$ ppm. The rate of H_2 gas supply required for maintaining the level of $C_H = 3.1$ ppm throughout the decarburization treatment is obtained to be 1.4 Nm^3/min.

An outline of the experimental procedures is shown in **Fig. 7**. The H_2 gas was fed in either by the bottom-blowing through porous bricks at the bottom of ladle or by blowing through the lance immersed in steel bath.

Changes in the hydrogen concentration in the course of the hydrogen blowing experiment are shown in **Fig. 8**. The amount of hydrogen blown in was 6–25 Nm^3, the average blow-in rate 0.5–1.0 Nm^3/min. Owing to the blowing of H_2 gas, the hydrogen concentration was held at a constant level of approximately 3–6 ppm until the later half of the treatment. Through the experiment of feeding hydrogen, it was

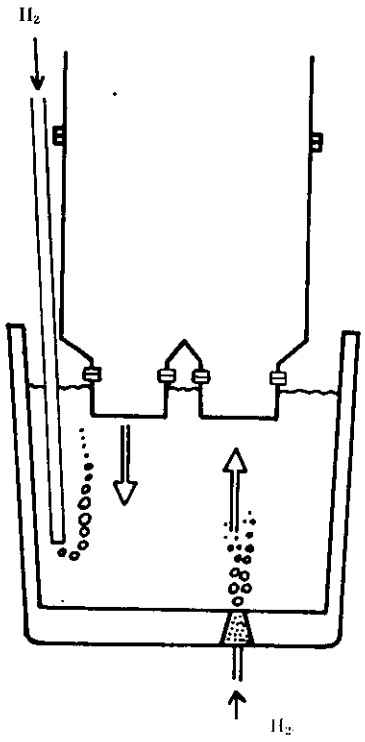

Fig. 7 Experimental method of hydrogen addition

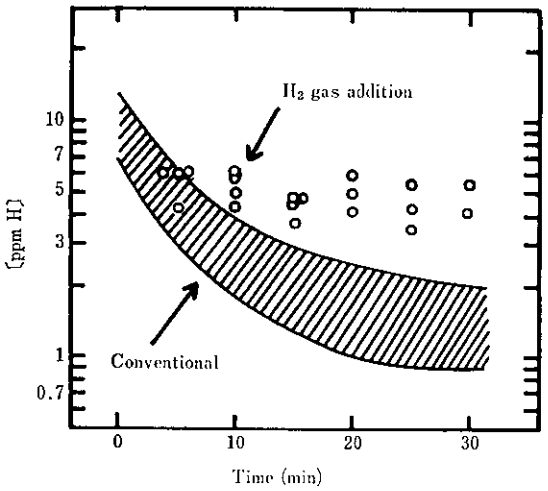

Fig. 8 Hydrogen concentration changes during decarburization

confirmed that the addition of hydrogen exerted significant effect by improving the apparent rate constant, K, of decarburization from area Ⅱ to area Ⅲ in **Fig. 2**. However, since hydrogen feeding revealed some problems with the stability of gas supply such as abnormal damage of porous bricks at the ladle bottom and the ageing of immersion lance, this method has not yet been put to the application in commercial production.

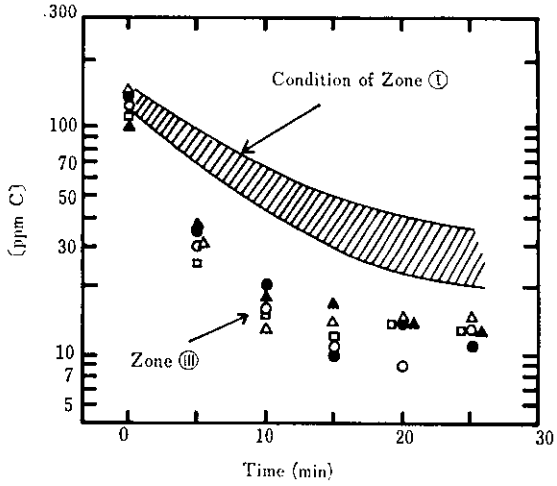

Fig. 9 Decarburization curves for conditions of zone Ⅰ and Ⅲ

3.2.3 Experiment for feeding argon gas into vessel

In parallel with the experiment for hydrogen feeding, argon gas was fed into the vacuum vessel at a rate of 500–1 000 N*l*/min for the same purpose of hydrogen feeding to improve the decarburization rate. While there were the problems of splashing increase in the vacuum vessel, and the wear of the lower part of the vacuum vessel and the bottom bricks, the rate constant of decarburization was also improved from Ⅱ to Ⅲ in the experiment for feeding argon gas as shown in **Fig. 2**. A representative decarburization curve for the experimental heat described above is shown in **Fig. 9**. Under the conditions of Ⅲ, it was found that the molten steel of 20 ppm or lower carbon concentration was obtained through the decarburization treatment for 10 min. which was a target time set at the start of the experiment.

4 Commercial Production of Ultra Low Carbon Steel

Since the start of operation of the continuous casting system in April 1981, the experiment of producing ultra-low carbon steel has been carried out at the No. 3 Steelmaking Shop, Chiba Works, and the commercial production has been under way since December 1981. The changes in the production of ultra-low carbon steel are shown in **Fig. 10**.

At the time of starting the production of ultra-low carbon steel, the RH treatment took about 40 min. and the temperature of steel tapped from the converter was higher than 1 680°C. However, as the decarburization rate was augmented as described in

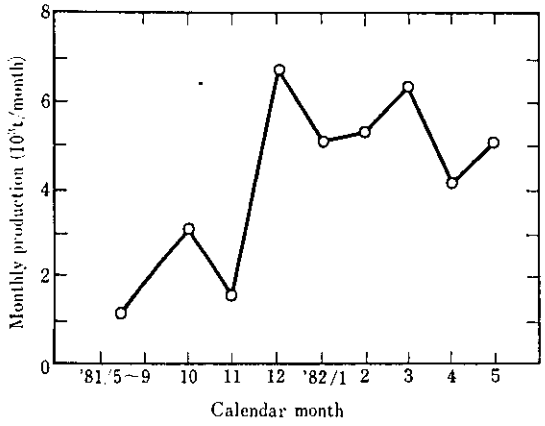

Fig. 10 Monthly production of ultra-low carbon steel at Chiba No. 3 Steelmaking Shop

the preceding section, the decarburization time was shortened to 10–15 min. and the RH treatment time was reduced extensively. Changes of the whole time for RH including the treatments for decarburization and for deoxidation and chemistry trimming are shown in **Fig. 11**. At present, the ultra-low carbon steel can be stably produced in a total treatment time of 24–25 min., allowing the continuous-continuous casting.

Since the RH treatment time was shortened as described above, the temperature of molten steel tapped from the converter was lowered extensively. In order to lower the tapping temperature further, aluminum was added to steel during tapping. As shown in **Fig. 12**, the addition of 0.4 kg/t Al can reduce the tapping temperature drop by about 10°C without affecting the RH decarburization treatment. Moreover, the aluminum added at the time of tapping effectively reduced the concentration of FeO in ladle slag to diminish the fluctuation in the yield of added aluminum in RH and in the changes of molten steel temperature, thus contributing to the stabilization of RH treatment.

Owing to the reduction of RH treatment time and the addition of aluminum at the time of tapping, as described above, the tapping temperature which had been required to be 1 680°C or higher initially, was reduced to 1 640°C as shown in **Fig. 13**, allowing the extension of the service life of refractory materials in the converter, ladle and RH.

Figure 14 shows the carbon concentration of recent ultra-low carbon steel products. In spite of reduced treatment time, the actual carbon concentration was 19.4 ppm on an average.

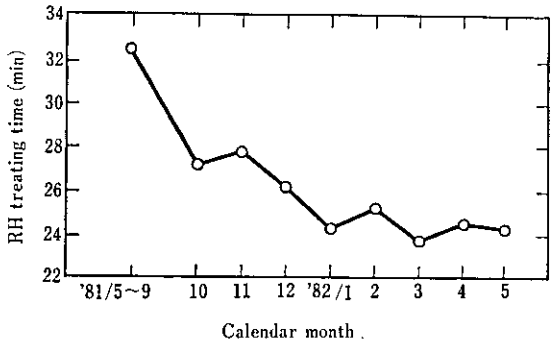

Fig. 11 Monthly change of RH treatment time

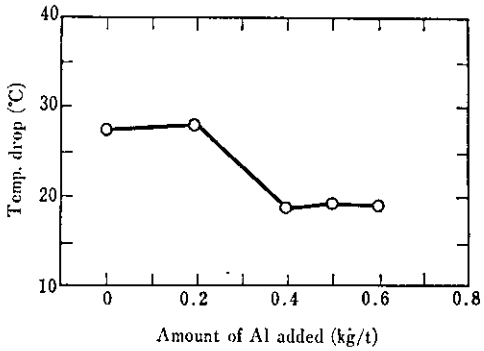

Fig. 12 Effect of Al addition on temperature drop during tapping

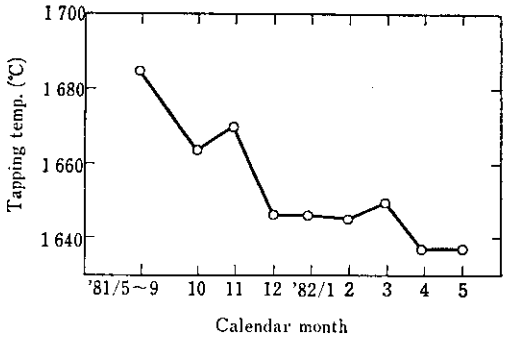

Fig. 13 Monthly change of tapping temperature at Q-BOP for ultra-low carbon steel

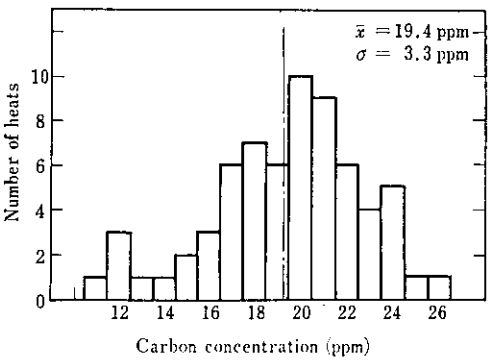

Fig. 14 Distribution of carbon concentration in products

5 Mechanical Properties of Ultra-Low Carbon Steel Produced by the New Method

The typical compositions of extra-deep drawing cold rolled steel sheet and deep drawing high strength cold rolled steel sheet produced through the process described above are shown in **Table 2.**

Generally, as the carbon concentration is reduced, drawability (Lankford value, $\bar{r}$) and elongation (El) increase, while tensile strength decreases. In the extra-deep drawing high strength cold rolled steel sheet shown in **Table 2**, the carbon concentration was reduced to 30 ppm or less to improve the elongation and drawability, niobium was added to secure non-aging properties by precipitating carbon and nitrogen as niobium carbide and niobium nitride, respectively, and phosphorus was added to augment tensile strength (TS). Since in a steel of such composition, the recrystallization temperature is high because of niobium content, and rapid cooling is required for preventing brittleness due to the intergranular segregation of phosphorus, it is difficult to make such steel through the batch annealing. The production of deep drawing high strength steel sheet of which mechanical properties were shown in **Table 3** was realized only with the multipurpose continuous annealing process which allowed rapid cooling at a rate of 40°C/s. The mechanical properties of deep drawing high strength cold rolled steel sheet produced in this way are shown in **Fig. 15**. The steel has lower yield point (YS), better ductility and $\bar{r}$-value greater than 2.0, in comparison with the conventional phosphor-added high strength cold rolled steel sheet. This steel is widely used as cold rolled steel sheet for automobiles of excellent press-formability.

6 Conclusions

The technique for an efficient production of ultra-low carbon steel of high quality was established through the process including bottom-blown converter, allowing a decarburization to the ultra-low carbon level, while suppressing the oxidation loss of iron, RH circulating vacuum degasser of high efficiency with increasing circulation and continuous casting system. The combination of this technique with the continuous annealing system (KM-CAL) contributes to the production of cold rolled steel strip having excellent mechanical properties, such as of extra-deep drawing steel sheets and deep drawing high strength steel sheets.

Table 2 An example of chemical composition of ultra-low carbon steels (%)

	C	Mn	P	S	Al	Nb
Extra deep drawing steel	0.0015	0.18	0.008	0.009	0.035	0.008
Extra deep drawing high strength steel	0.0017	0.23	0.065	0.008	0.040	0.016

Table 3 Mechanical properties of extra-deep drawing high strength steel sheets 0.7 mm in thickness shown in Table 2

YS (kgf/mm²)	TS (kgf/mm²)	El (%)	YR (%)	$\overline{n}$	$\overline{r}$
19.4	35.5	44.1	54.7	0.250	2.15

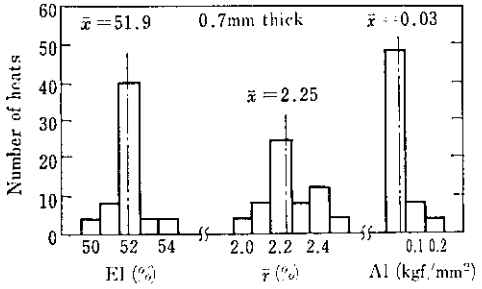

Fig. 15 Distributions of elongation (El), the Lankford value, $\bar{r}$, and annealing index, AI, of extra-deep drawing steel strip continuously annealed

References

1) K. Yoshimura, N. Sumida, T. Fujii, F. Sudo and Y. Oguchi: *Proc. 7th ICVM* (1982), Tokyo, Japan, p. 1 404
2) A. Ejima, Y. Oguchi, T. Fujii, N. Sumida, Y. Iida, N. Shimazaki and N. Ueda: *Tetsu-to-Hagané*, **61** (1975) 12, S543
3) H. Watanabe, K. Asano and T. Saeki: *Tetsu-to-Hagané*, **54** (1968) 13, p. 1 327
4) H. Matsunaga, T. Tominaga, M. Ohji and F. Tanaka: *Tetsu-to-Hagané*, **63** (1977) 13, p. 1 945
5) F. Tanaka, M. Sakakibara and J. Hayashi: *Seitetsu Kenkyu*, (1978) 293, p. 49
6) K. Kinoshita and K. Nakanishi: *Tetsu-to-Hagané*, **57** (1971) 11, S419
7) N. Sumida, K. Saito, Y. Oguchi, K. Komamura and T. Yamamoto: *Tetsu-to-Hagané*, **66** (1980) 4, S130
8) H. Mass: *Rev. Metall.*, **60** (1963), p. 421